

# Jahn-Teller effect on exciton states in hexagonal boron nitride single crystal

Kenji Watanabe\* and Takashi Taniguchi

National Institute for Materials Science, Namiki 1-1, Tsukuba, Ibaraki 305-0044, Japan

(Received 13 March 2009; published 21 May 2009)

Optical properties near the band edge of hexagonal boron nitride were studied at 8 K. The photoluminescence spectrum shows two series of bands, namely, sharp (S) and diffuse (D), which are also distinguished by their fast (0.6 ns) for S and slow (5 ns) for D radiative decay time. Each series is composed of four bands with large Stokes shifts that are attributed to self-trapped excitons by the strong exciton-phonon interaction. The respective four luminescence bands of the two series originate from the four free-exciton levels in which the doubly degenerated dark and bright exciton levels theoretically predicted are resolved with the Jahn-Teller distortion in the excited states.

DOI: 10.1103/PhysRevB.79.193104

PACS number(s): 71.35.Aa, 71.70.Ej, 78.20.-e

The highly luminous exciton properties of hexagonal boron nitride (*h*BN) in the far ultraviolet region have been a significant issue in both theoretical and experimental approaches. A Wannier exciton model was proposed with an experimental study of the optical properties of a pure single crystal.<sup>1</sup> On the contrary, successive theoretical works reported that the electronic structure near the band edge is governed by either the Frenkel or charge transfer types of excitons.<sup>2-6</sup> The latest theoretical calculations predict that the exciton with the largest oscillator strength (bright exciton), which is a dipole-allowed transition, is located at 6.1 eV while the dark exciton, which is a dipole-forbidden transition, is located at an energy slightly lower than the bright exciton energy.<sup>3,5</sup> In addition to this forbidden band, there are some spin-triplet states at a somewhat lower energy than that of the optically active 6.1 eV band,<sup>4,6</sup> hence those excitons, including the optically active 6.1 eV band, do not play a major role in the active luminescence. For this reason, these theories conclude that the practical luminous properties of *h*BN are attributed to either the extrinsic effects caused by imperfections of the crystal, such as impurities or dislocations, which would cause intersystem crossing or similar,<sup>5</sup> or the mechanism in which the large oscillator strength of the bright exciton at 6.1 eV is partly provided to the dark exciton band as a result of the zero-point vibration of the lattice.<sup>3,7</sup>

However, the luminous property of a pure *h*BN crystal is less likely to be caused by such second-order effects because of the crystal's high-luminous efficiency.<sup>1,8,9</sup> From our previous experience, the calibrated excitonic luminescence intensity for pure single crystals is comparable to that for pure ZnO single crystals of several percentages of the internal quantum efficiency, hence *h*BN shows as high-luminous efficiency as other direct-gap semiconductors. Thus, clear explanation based on detailed experiments of the optical properties, including excitonic luminescence, is necessary to overcome the disagreement between these theories and experiments.

We studied the optical properties of *h*BN at 8 K and report that our previous work<sup>1</sup> is in need of major revision to describe the electronic properties of *h*BN near the band edge. The most intense excitonic luminescence bands are attributed to the lowest dipole-allowed Frenkel excitons with a large Stokes-energy shift, which suggests that the excitons are self-trapped by their strong interaction with phonon. We also

report the relationship between the absorption bands at around 5.8 eV and deformation of the crystal and show that these bands are induced by deformation, which is contrary to our previous model of the Wannier exciton. We finally reveal that the spontaneous symmetry breaking caused by dynamic Jahn-Teller distortion in the exciton states resolves the disagreement between the theories and experiments.

Pure *h*BN crystals were grown using a previously reported method.<sup>1,10</sup> Since simple deformation of a transparent crystal forms stacking faults<sup>11,12</sup> and affects the luminescence properties and also the absorption spectra, transparent samples were carefully cleaved from the as-grown bulk crystals containing many striae so as to remove visible stacking faults from the samples.

The photoluminescence was excited with the fourth harmonics of a Ti: sapphire laser of 198 nm. Time-resolved-photoluminescence measurements were carried out using a time-correlated single-photon counting technique with a 30 ps resolution. The details of the experimental setup have been already reported.<sup>13</sup> The absorption and reflectance spectra were obtained using a deuterium lamp. The samples were cooled at 8 K using a He refrigerator.

Figure 1 shows an example of the temperature dependence of the photoluminescence spectra from 7.6 to 280 K. A

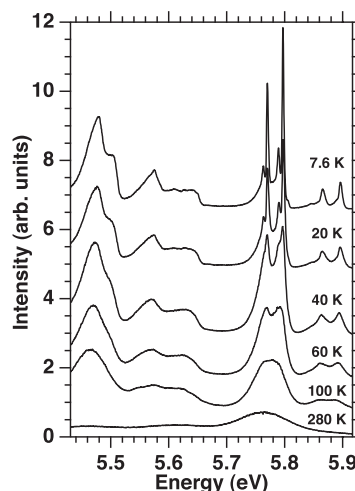


FIG. 1. Example of temperature dependence of photoluminescence spectra from 7.6 to 280 K.

dominant 5.765 eV (215 nm) band was observed at 280 K. This 5.765 eV band shows complicated fine structures below 20 K accompanied by sharp structures at 5.865 and 5.896 eV. When the sample temperature decreased, broad bands from 5.4 to 5.7 eV appeared. These broad bands are related to the stacking faults described above. Although the visible stacking faults were carefully removed and the sample position, where no obvious defect bands appeared, was selected at room temperature, relaxation processes at low temperature enabled those low-lying defect states to be populated and to show the emission. In this manner, the photoluminescence spectroscopy is a sensitive method for studying the defect of *h*BN.

The photoluminescence bands can be clearly classified into two series based on the bandwidth, which are denoted by S (sharp series) and D (diffuse series) in Fig. 2(c). The energy spacings in each series have a fixed pattern. By shifting the energy of the D series by 290 meV the structures from D1 to D4 show a one-to-one correspondence to those from S1 to S4 except for the doublet of S3 and S4 bands.

Classification of S and D series is also possible based on their decay time. The sharp line series from S1 to S4 shows a decay time of 0.6 ns while the D series from D1 to D4 shows a slower decay time of 5 ns. All the bands show a single exponential decay and the decay time can be estimated by a single exponential fit.

The luminescence intensity of the broad D series increases when the *h*BN single crystal is deformed and stacking faults are introduced.<sup>11,12</sup> The sample with thickly distributed striae after deformation showed a strong D series while the carefully cleaved samples before deformation, which were completely transparent to the eyes, predominantly showed an intense S series at room temperature. The correlation between the D4 luminescence band and the absorption band of 5.8 eV was recently pointed out by *Museur et al.*,<sup>14,15</sup> though this absorption band was previously assigned to a 1s Wannier exciton band in our previous paper.<sup>1</sup>

To clarify the relationship between deformation and the electronic structure, we compared the absorption spectra before and after deformation and then examined the relationship between the absorption and luminescence bands. The deformation process was done by dropping a 57 g indenter with a 0.3 mm  $\phi$  in diameter tip to a carefully cleaved transparent sample from a height of 1 cm. The sample size was almost the same as that of the tip. This process changed the transparent sample into a striae-rich one with the sample thickness remaining almost unchanged.

The absorption spectra are shown in Fig. 2(a). The dotted line is the absorption spectrum before deformation and the solid line is the one after deformation. The new bands appeared at energies of 5.800, 5.825, 5.890, and 5.928 eV after deformation. At the same time, we observed that the luminescence spectrum was dominated by the D series of the broad structures. As a result, the series of absorption bands from 5.800 to 5.928 eV is attributed to the excitonic states induced by the stacking faults rather than to the series of Wannier excitons. Since the energy sequence of the photoluminescence series from D1 to D4 corresponds well to the absorption series formed by deformation we can assign the respective luminescence bands to the absorption origin. The

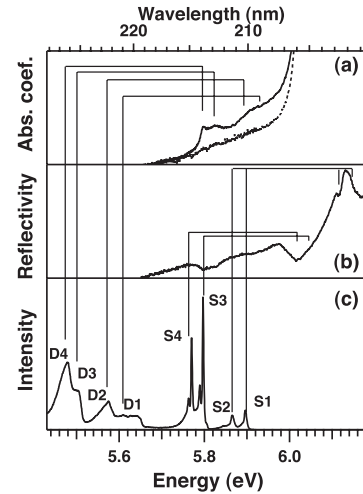


FIG. 2. (a) Absorption, (b) reflectance, and (c) photoluminescence spectra for high purity *h*BN at 8 K. In spectra (a), dotted line indicates spectrum before deformation and solid line indicates one after deformation. Spectra (b) and (c) were obtained from transparent single crystals. Structure at 5.8 eV in (b) arose from rough-edged region of clear sample.

lines from the D series to the absorption bands in Figs. 2(a) and 2(c) denote this correspondence. The Stokes shift for respective luminescence bands in the D series shows almost the same energy of 319 meV, which is larger than the largest phonon energy of 200 meV.<sup>16</sup> This large Stokes shift suggests that the excitons form self-trapped states due to the strong interaction with the lattice distortion.<sup>17</sup> Similar assignments between the luminescence and reflectance spectra are also possible for the sharp S lines as described below.

Since the energy spacings of the bands in the S series are the same as the ones in the D series and there is no absorption band corresponding to the energy of the S series except for those at around 5.8 eV that are induced by the deformation described above, we can assume a similar Stokes-shift energy for the S series. Because the absorption coefficient estimated from the transmission spectrum above 6.0 eV was over the range for our measurement system we carried out a reflectance measurement and compared the results with the S series luminescence bands. The corresponding reflectance structures for the photoluminescence bands from S1 to S4 are indicated by the lines between the luminescence and reflectance bands in Figs. 2(b) and 2(c). The structural energy positions of the reflectance spectrum were estimated by differentiating the reflectance spectrum.

Figure 3 displays a summary of the electronic structure derived from the reflectance and absorption spectra and the related luminescence bands with the theoretical results from *Arnaud et al.*<sup>2</sup> The energy diagram of the experimental results is different from the one from recent theoretical results where one bright exciton is accompanied by a dark exciton, which is at a slightly lower energy than that of the bright one<sup>3,5</sup> and resembles the diagram by *Arnaud et al.*<sup>2</sup>; the four excitonic states near the band-edge region show the largest oscillator strength. However, this model has a symmetry problem. *Wirtz et al.*<sup>3,5</sup> suggested that threefold-rotation symmetry changes the four discrete levels to doubly gener-

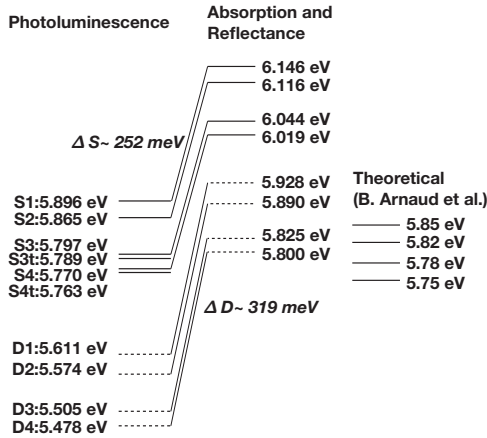


FIG. 3. Summary of electronic structure derived from reflectance and absorption spectra and corresponding luminescence bands with theoretical calculation by Arnaud *et al.* (Ref. 2).  $\Delta S$  and  $\Delta D$  denote Stokes-shift energy.

ated dark and bright exciton levels. Thus only one optically active bright-exciton band should be expected near the band edge according to the latest model.

We introduced the Jahn-Teller effect to the excited states to consistently explain the experimental and theoretical results. According to the Jahn-Teller theorem,<sup>18</sup> the generalized force  $F_k$  on a nucleus is

$$F_k = \langle i | \partial V / \partial Q_k | i \rangle, \quad (1)$$

where  $|i\rangle$  is the electronic state,  $V$  is the total potential energy, and  $Q_k$  is the coordinate. Following the elementary group theory  $F_k$  can be nonzero for the lowest exciton level with the shear deformation of the two facing chicken-wire layers in its unit cell as follows. Assuming that the lowest exciton symmetry is doubly degenerated  $E_{2u}(x, y)$  and simplifying the direct product of  $E_{2u}(x, y)$ , we obtain the irreducible expressions of  $A_{1g} + A_{2g} + E_{2g}$ . Since the irreducible expression for phonons at the Brillouin zone center can be derived as  $2E_{1u} + 2A_{2u} + 2E_{2g} + 2B_{1g}$ ,<sup>16</sup> the Jahn-Teller distortion of the  $E_{2g}$  type is possible in the excited states of  $hBN$ . Two types of  $E_{2g}$  modes are possible for the Jahn-Teller effect removing the degeneracy of the exciton states. One of the  $E_{2g}$  representations corresponds to the phonon mode of the shearing between the two facing  $sp^2$  chicken-wire layers composed of boron and nitrogen atoms, and the other is the mode in which respective boron and nitrogen atoms in plane move in the opposite direction as the facing atoms between the layers move in the same phase. The energy of the former shear mode is quite small, 6 meV, reflecting the weak interaction between the layers and the latter is 170 meV. Thus, the dynamic Jahn-Teller distortion accompanied by the low-energy shear mode is a possible model for explaining the symmetry breaking.<sup>18</sup> By the shearing distortion, the crystal symmetry  $D_{6h}$  reduces to  $C_{2h}$ , which does not have a threefold-rotation symmetry. By this means, the calculated results by Arnaud *et al.*<sup>2</sup> are justified in the symmetric argument. The violation of the symmetry due to the Jahn-Teller distortion can change two doubly generated bright and dark exciton levels to four subpeaks from 5.7 to 5.9 eV which

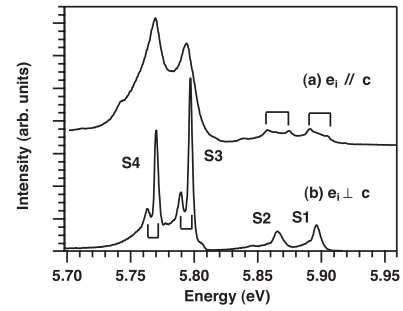


FIG. 4. Incident polarization dependence of photoluminescence spectra. (a) S1 and S2 bands show split for incident polarization parallel to  $c$  axis and incident and output vectors perpendicular to  $c$  axis, (b) S3 and S4 bands show split for incident polarization perpendicular to  $c$  axis, and incident and output vectors parallel to  $c$  axis. Spectrum (a) shows broader bands than spectrum (b) owing to rough-edged region of clear sample on which excitation light was incident.

correspond to our experimentally obtained structures from 6.019 to 6.146 eV (Fig. 3).

This assumption was qualitatively and quantitatively confirmed using polarization measurements. Figure 4 shows the photoluminescence spectra for two incident polarization configurations. The component parallel to the  $c$  axis is dominantly excited in the excitation configuration (a) while the component perpendicular to the  $c$  axis is dominantly excited in configuration (b). Spectrum (a) shows the split in the S1 and S2 bands while spectrum (b) indicates the split in the S3 and S4 bands. The splitting energies are different for each band: 14 meV for S1, 17 meV for S2, 8 meV for S3, and 7 meV for S4 bands. Assuming the Jahn-Teller distortion of  $E_{2g}$  mode, the doubly degenerated  $E_{2u}(x, y)$  exciton level corresponds to the symmetry of  $A_u(x) + B_u(y, z)$  by the adaptation relation from  $D_{6h}$  to  $C_{2h}$ . Thus, the split of each band can be assigned to the transverse and longitudinal (T/L) components of the Frenkel excitons; the S1 and S2 split bands in spectrum (a) can be assumed as  $B_u$ -like symmetry and the S3 and S4 split bands in spectrum (b) as  $A_u$ -like symmetry. By using the split energy of the T/L split bands, we can estimate the dipole moment of the exciton levels and hence the oscillator strength.<sup>19</sup> The derived exciton oscillator strength per exciton is shown in Fig. 5. This experimental result almost reproduces the relative relationship of the oscillator strengths theoretically estimated by Arnaud *et al.*<sup>2</sup> except for their absolute energy positions.

The large Stokes shift of the S series of the luminescence bands suggests the self-trapped exciton due to the large exciton-phonon interaction.<sup>20</sup> In practice, the temperature dependence of the absorption tail of  $hBN$  followed the Urbach rule which indicates the exciton-phonon interaction. The Urbach rule shows that the exciton absorption spectra  $F$  depends on the energy  $E$  at temperature  $T$  as following:

$$F(E) \propto \exp\left(-\sigma \frac{E'_0 - E}{k_B T}\right), \quad (2)$$

where  $\sigma$  is a dimensionless steepness coefficient,  $E'_0$  is the converging point of the semilogarithmic plots of the absorp-

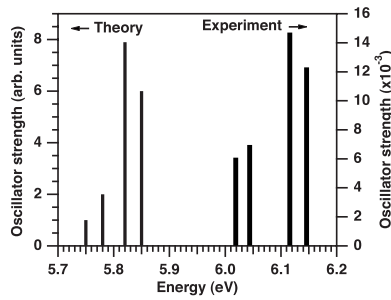


FIG. 5. Experimental and theoretical values of oscillator strength. Theoretical values were normalized to their lowest energy level at 5.75 eV (Ref. 2).

tion spectra at various temperatures, and  $k_B$  is the Boltzmann factor. Figure 6 shows the semilogarithmic plot of the absorption tail from 220 to 320 K. As shown in the figure, the exciton absorption spectra depend exponentially on the energy ranging from 5.8 to 5.9 eV. The convergence energy  $E'_0=6.127$  eV and the steepness constant  $\sigma=0.5$  were obtained from the fit using Eq. (2). This convergence energy of 6.127 eV is located in the region where the largest oscillator-strength excitons are distributed. The convergence energies lower than 200 K were scattered in consequence of the superposition of the sharpened discrete exciton absorption tails with a large oscillator strength. Using the exciton-phonon interaction constant  $\sigma=s/g$  defined by Toyozawa,<sup>20</sup> the exciton-phonon interaction constant of  $g=3.0$  was estimated from the fitted value of  $\sigma=0.5$  and the assumed steepness index of  $s=1.5$ .<sup>20</sup> This exciton-phonon interaction constant far exceeds  $g=2.0$  for alkali halides indicating a large exciton-phonon interaction.<sup>20</sup> This large exciton-phonon interaction is also able to cause photoinduced change in the *h*BN structure similar to that in alkali halides. In fact, the pulse excitation density of several MW/cm<sup>2</sup> at 198 nm for several minutes changed the luminescence spectra from S series to the dominant D series evidently forming the stacking faults.

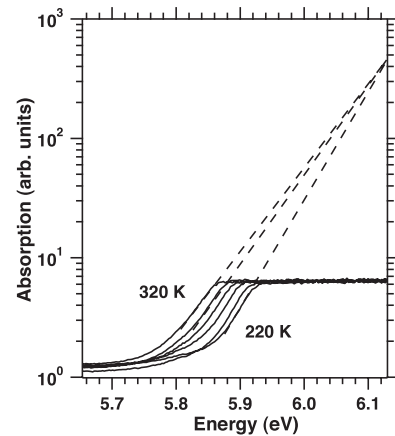


FIG. 6. Urbach tails for *h*BN. Dashed lines are fitted results. Plateaus in each spectrum indicate dynamic-range limit of our direct-absorption measurement system.

In summary, we have directly compared the theoretical results from Arnaud and Wirtz<sup>2-5</sup> with experimental ones and revealed that the optically activated four exciton states are produced from the dynamic Jahn-Teller effects, which solve the degeneracy of bright and dark exciton levels. The large Stokes shift of the exciton luminescence bands indicates that the strong exciton-phonon interaction causes self-trapped exciton states. The strong luminous properties originate from those self-trapped exciton states.

We gratefully acknowledge T. Kuroda and K. Kobayashi for their fruitful discussions. This research was partially supported by the Ministry of Education, Culture, Sports, Science, and Technology (MEXT), Japan, Grants-in-Aid for Scientific Research (A) under Grant No.19205026, 2007 and on priority areas “Nano Materials Science for Atomic Scale Modification 474.”

\*watanabe.kenji.aml@nims.go.jp

- <sup>1</sup>K. Watanabe, T. Taniguchi, and H. Kanda, *Nature Mater.* **3**, 404 (2004).
- <sup>2</sup>B. Arnaud, S. Lebègue, P. Rabiller, and M. Alouani, *Phys. Rev. Lett.* **96**, 026402 (2006).
- <sup>3</sup>B. Arnaud, S. Lebègue, P. Rabiller, and M. Alouani, *Phys. Rev. Lett.* **100**, 189702 (2008).
- <sup>4</sup>L. Wirtz, A. Marini, M. Grüning, and A. Rubio, arXiv:cond-mat/0508421 (unpublished).
- <sup>5</sup>L. Wirtz, A. Marini, M. Grüning, C. Attaccalite, G. Kresse, and A. Rubio, *Phys. Rev. Lett.* **100**, 189701 (2008).
- <sup>6</sup>K. Harigaya, *J. Exp. Theor. Phys.* **97**, 1246 (2003).
- <sup>7</sup>A. Marini, *Phys. Rev. Lett.* **101**, 106405 (2008).
- <sup>8</sup>K. Watanabe, T. Taniguchi, and H. Kanda, *Phys. Status Solidi A* **201**, 2561 (2004).
- <sup>9</sup>Y. Kubota, K. Watanabe, O. Tsuda, and T. Taniguchi, *Science* **317**, 932 (2007).
- <sup>10</sup>T. Taniguchi and K. Watanabe, *J. Cryst. Growth* **303**, 525 (2007).
- <sup>11</sup>K. Watanabe, T. Taniguchi, T. Kuroda, and H. Kanda, *Appl.*

*Phys. Lett.* **89**, 141902 (2006).

- <sup>12</sup>K. Watanabe, T. Taniguchi, T. Kuroda, and H. Kanda, *Diamond Relat. Mater.* **15**, 1891 (2006).
- <sup>13</sup>K. Watanabe, T. Taniguchi, T. Kuroda, O. Tsuda, and H. Kanda, *Diamond Relat. Mater.* **17**, 830 (2008).
- <sup>14</sup>L. Museur, E. Feldbach, and A. Kanaev, *Phys. Rev. B* **78**, 155204 (2008).
- <sup>15</sup>L. Museur and A. Kanaev, *J. Appl. Phys.* **103**, 103520 (2008).
- <sup>16</sup>J. Serrano, A. Bosak, R. Arenal, M. Krisch, K. Watanabe, T. Taniguchi, H. Kanda, A. Rubio, and L. Wirtz, *Phys. Rev. Lett.* **98**, 095503 (2007).
- <sup>17</sup>Y. Toyozawa, *J. Lumin.* **24-25**, 23 (1981).
- <sup>18</sup>M. D. Sturge, in *Solid State Physics* 20th ed., edited by F. Seitz, D. Turnbull, and H. Ehrenreich (Academic Press, New York, 1964), p. 91.
- <sup>19</sup>E. S. Koteles, in *EXCITONS*, edited by E. I. Rashba and M. D. Sturge (North-Holland Publishing Company, Amsterdam, New York, Oxford, 1982), p. 83.
- <sup>20</sup>M. Schreiber and Y. Toyozawa, *J. Phys. Soc. Jpn.* **51**, 1544 (1982).